Measurement of X-ray photon energy and arrival time using a silicon drift detector[*]

LIU Li(刘利)   YU Hai(郁海)   ZHENG Wei(郑伟)[1)]

College of Aerospace Science and Engineering, National University of Defense Technology, Changsha 410073, China

Abstract: Detecting the X-ray emission of pulsars and obtaining the photons' time of arrival are the foundational steps in autonomous navigation via X-ray pulsar measurement. The precision of a pulse's time of arrival is mainly determined by the precision of photon arrival time measurement. In this work, a silicon drift detector is used to measure photon energy and arrival time. The measurement system consists of a signal detector, a processing unit, a signal acquisition unit and a data receiving unit. This system acquires the energy resolution and arrival time information of photons. In particular, background noise with different energies disturbs pulse profile forming, the system can also achieve a high signal-to-noise ratio profile. Ground test results show that this system can be applied in autonomous navigation based on X-ray pulsar measurement.

Key words: X-ray photon energy, time of arrival, detector

PACS: 29.40.Vj   **DOI:** 10.1088/1674-1137/38/3/036003

1 Introduction

X-ray pulsar navigation has been a research hotspot for several years and is a novel autonomous navigation approach to the operation of satellites. Related papers mainly concentrate on X-ray pulsar observation [1], detectors and navigation theory [2, 3]. A series of science programs has also been carried out for X-ray pulsar navigation [4]. Based on the characteristics of X-ray pulsar navigation, the requirements for X-ray pulsar detection are as follows. First, the detection energy should range from 1 keV to 10 keV. Second, the detection requires sufficient energy resolution to eliminate background noise. Third, the detection time resolution should be better than or equal to 10 μs.

The most common detection types are gas proportional counters, micro-channel plates (MCP) and semiconductor detectors. Gas proportional counters are limited due to the gas lifetime and damage to the anode wires within the chambers [5]. Although MCPs have a high time resolution, they do not have good energy resolution [6]. A silicon drift detector (SDD) is a kind of semiconductor detector. An SDD is unique and practical because it simultaneously achieves high energy resolution and fast timing compared with conventional semiconductor detectors. An SDD can also be used at near-room temperatures [7]. In an autonomous navigation-based pulsar field, an SDD can provide precise X-ray photon energy and time information.

2 Structure of measurement system of photon energy and arrival time

2.1 Overall structure of the system

The system consists of four parts: an X-ray detector and signal processing unit, a photon energy and photon time of arrival acquisition unit, a data receiving unit and a power supply system. In the X-ray detector and signal processing unit, the charge signal generated from the SDD detector goes through a four circuit module including a charge-sensitive amplifier, filter and shaper circuit, pole-zero cancellation and the main amplifier, which transforms the signal into a near-Gaussian shape. In the photon energy and photon time of arrival acquisition unit, a Gaussian analog signal is transformed to a numerical signal. The energy and time information of the numerical signal is then captured by an FPGA in this unit. Then, in the data receiving unit, data are transferred through the USB bus to the main computer. In the signal processing unit, the power supply system generates +12, −12, +5 and 1.3 V. The acquisition unit requires +12, −12 and +5 V.

2.2 SDD unit

As shown in Fig. 1 [8], an SDD consists of fully depleted high-resistivity silicon, in which an electric field

parallel to the surface and created by properly biased contiguous field strips drives signal charges toward a collecting anode. A front-end n-channel junction gate field-effect transistor is integrated onto the detector chip close to the n+ implanted anode. The extremely low anode capacitance enables higher resolution for a short shaping time. The X-ray detector efficiency is about 100% at 10 keV and 75% at 2 keV with a 25 μm-thick beryllium window [9].
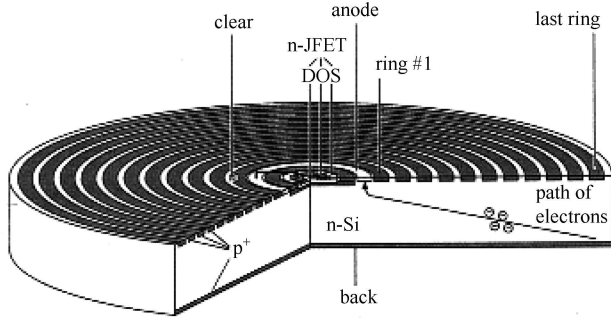

Fig. 1.   Cross-section of a cylindrical SDD.

2.3   Acquisition unit for X-ray photon energy and time of arrival

The acquisition unit for X-ray photon energy and arrival times is shown in Fig. 2. This unit contains a peak-holder circuit, event-choosing circuit, analog-to-digital conversion chip and FPGA chip. The FPGA is the core control chip that performs acquisition. The main function of this chip is to receive instructions from the main computer, control a single acquisition and send data back to the main computer through the USB bus.
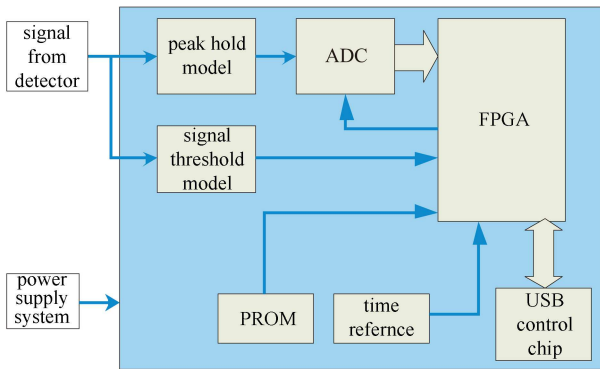

Fig. 2.   Electronic block diagram of the acquisition unit for photon energy and arrival time.

The acquisition unit flowchart is shown in Fig. 3. The unit enables the peak hold module to capture and hold the peak value of the signal. If the signal amplitude is higher than the threshold of the discriminator, the ADC circuit is trigged by the FPGA and starts to sample the

peak. The signal peak is considered equivalent to the signal energy.

As the ADC circuit is triggered, the signal's rising edge time is simultaneously captured by the FPGA, which is recorded by the interior counter and converted to absolute time by the crystal oscillator and multiplier in the FPGA. Energy and time information is stored in the FIFO unit. When the FIFO is full, the USB control module is used to send information to the upper computer and clean the FIFO. A data packet is comprised of eight bytes. The first byte is the prefix, the signal time information is in the second to sixth bytes, while energy information is in the remaining bytes.
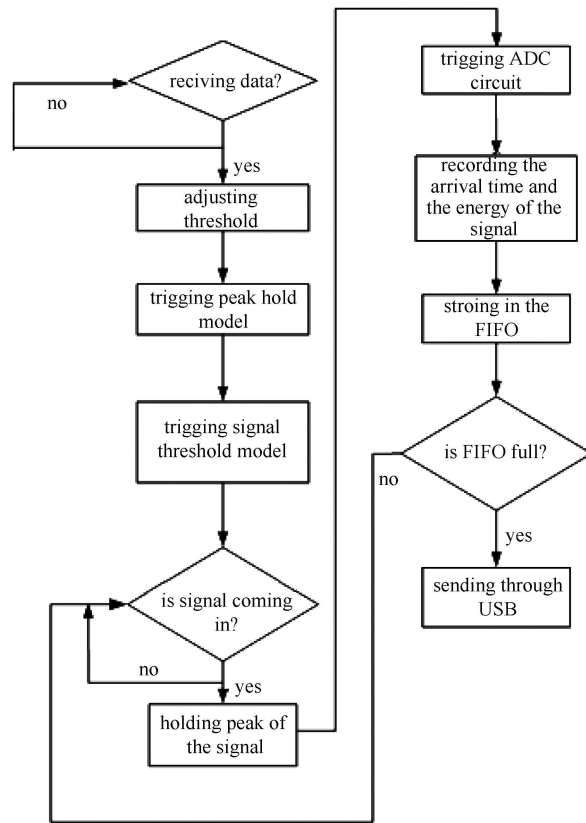

Fig. 3.   Flowchart of the acquisition unit.

3   Performance test

3.1   Energy resolution and energy linearity test

To determine the relationship between channels and photon energy, the energy spectrum lines of ^{55}Fe and ^{241}Am radioactive sources are measured to calibrate the linear energy.   Based on the measurement data in Table 1, the linear formulas can be expressed as $E=0.00766C+0.1446$, where C is the channel value and E is the corresponding energy (in keV). It is concluded

that the channel-to-energy relationship is almost perfectly linear, with a correlation coefficient of >0.99 and an integral nonlinearity (INL) of 1.05%.

To test the energy resolution performance of the SDD, ^{55}Fe and ^{241}Am source energy spectra are obtained. Fig. 4 shows that the energy resolution (FWHM) is around 155 eV@5.90 keV and 205 eV@13.93 keV.

Table 1.   Peak energy spectrum.

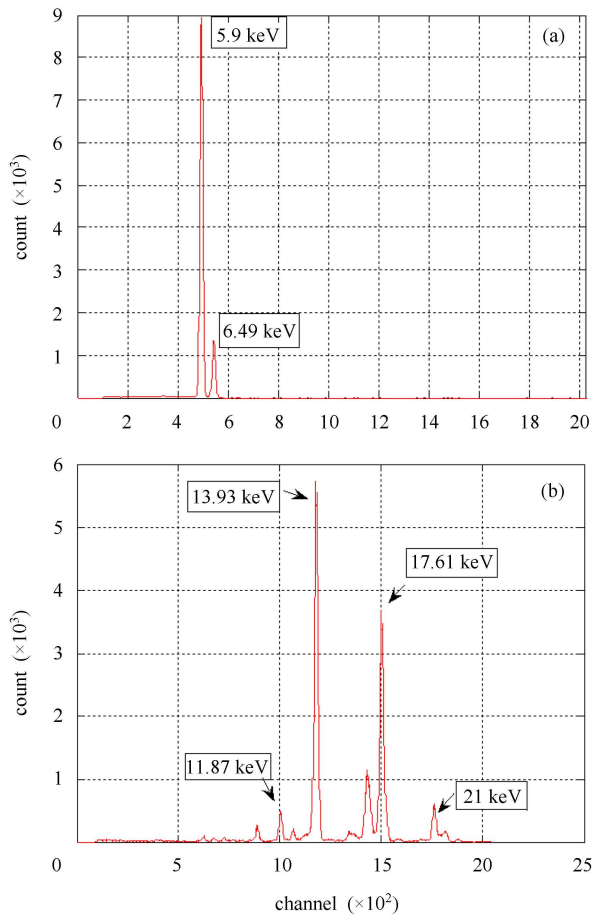| source	channel	energy/keV
^{55}Fe	492	5.90
	543	6.49
^{241}Am	1006	11.87
	1181	13.93
	1503	17.61
	1764	21.00

Fig. 4. (a) ^{55}Fe energy spectrum (FWHM ∼155 eV); (b) ^{241}Am energy spectrum (FWHM ∼205 eV).

3.2   Time precision and time resolution test

Time precision test

The time precision of the signal processing and acquisition units is a crucial factor affecting the time precision of the entire system. The time information of the signal pulses, which are assumed to be Gaussian, is collected using the signal processing and acquisition units. A signal generator is used to produce Gaussian pulses with 5 kHz frequency to substitute for the detector. The result of the time precision test is shown in Fig. 5. Most pulses are received at 200 μs (5 kHz). Only a few pulses have errors, and the RMS is 20.3 ns.
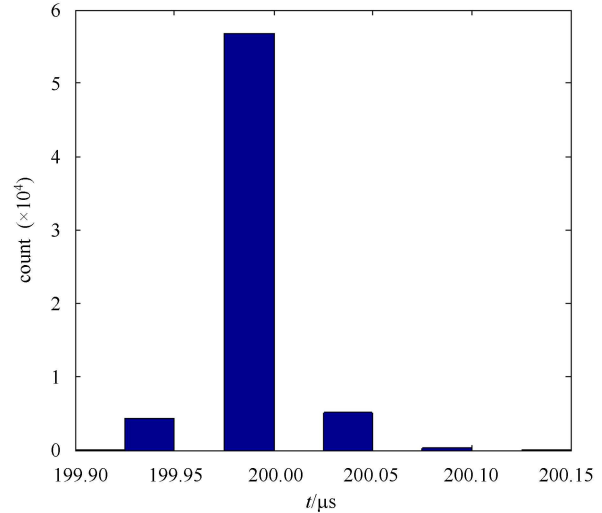

Fig. 5.   Time data collected by the acquisition units when the pulse frequency is 5 kHz.

Time resolution test

The time resolution of the SDD has a significant effect on navigation applications, and indicates the minimum time interval between two photons received by the detector. In the pulsar navigation application, the time resolution of the detector must be ⩽10 μs. The statistical distribution of the time interval of two photons is presented in Fig. 6(a). As shown in Fig. 6(b), the distribution of time intervals, shown with a logarithmic scale, fits an exponential distribution. Fig. 6(c) is an amplification of Fig. 6(a) (top). The minimum time interval of two photons is about 10 μs; that is, the detector's time resolution is 10 μs.

3.3   Pulse profile with background noise

Background noise is created by interactions between the detector and orbital environment particles, such as γ-rays, protons and electrons. Background noise decreases the pulse profile signal-to-noise ratio (SNR) and the precision of pulse time of arrival (TOA) estimation. The background energy spectrum differs from the X-ray photon signal energy, however, so the SDD energy resolution can be used to eliminate background noise.

To validate this idea, some experiments have been developed. First, X-ray pulses with low energy and background noise with high energy are produced. Second,

pulses with mixed arrival times, and background noise with and without energy information, are likewise produced. Finally, the effect of energy resolution on the pulse SNR is analyzed.
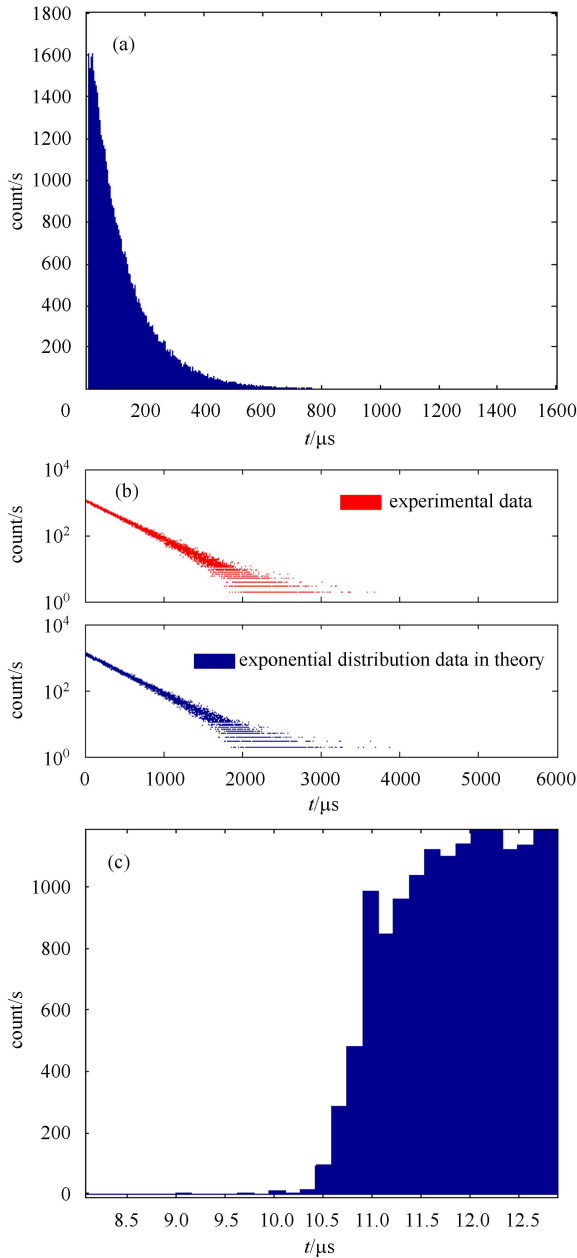

Fig. 6.   (a) Statistical distribution of time intervals; (b) exponential distribution of time intervals, with logarithmic scale; (c) system time resolution.

Pulse profile with low energy

Signal simulation [10], including X-ray source and profile modulation, is performed to produce periodic X-ray pulses and background noise. X-ray pulsar energies range from 1 keV to 8 keV, while Ti X-ray energies range

from 4 keV to 5 keV. Therefore, X-rays generated from an X-ray tube were used to bombard Ti to produce the right energy range for simulating an X-ray pulsar.

When the incident energy to the system is 10 keV and the period of the pulses is 25 ms, photon energy is produced (Fig. 7(a)). The main features of the energy spectrum are as follows: the Ti Kα characteristic line at 4.51 keV; the Ti Kβ characteristic line at 4.93 keV; and bremsspectrum, <10 keV.

The pulse profile made by combining 3000 pulse periods is shown in Fig. 7(b). Photon flow density in the peak is about 700 counts/s. Over five minutes, the detector received 38589 photons as a useful signal. No noise photons were received by the detector, so the photon flow density of the rest is zero.
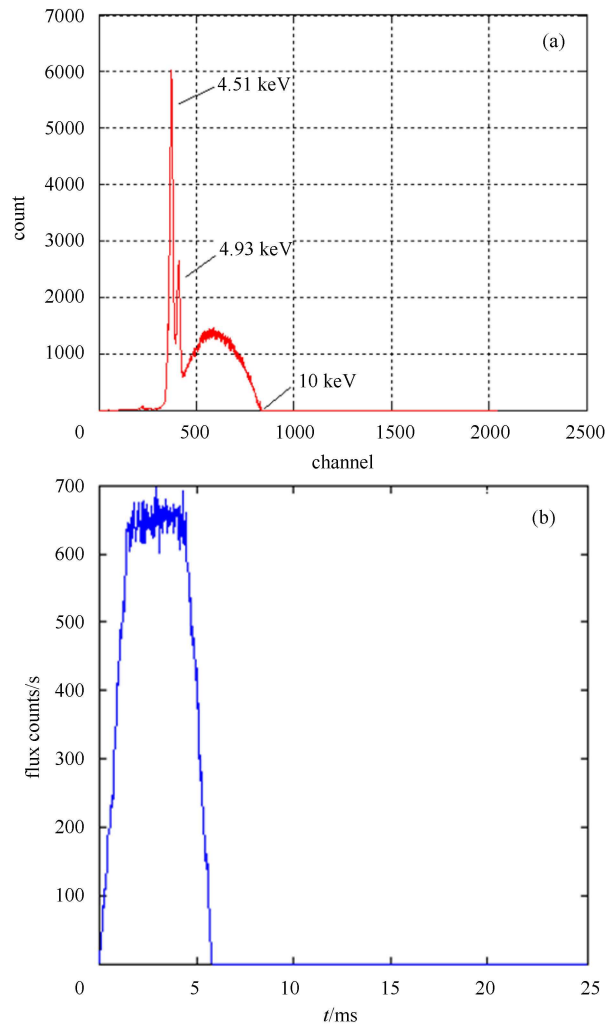

Fig. 7.   (a) Energy spectrum of pulse; (b) Pulse profile.

X-ray photon background noise

The Cu energy range is distributed within 8–9 keV. Therefore, X-rays generated from an X-ray tube were used to bombard Cu to produce the right energy range

to simulate background noise. Over five minutes, the detector received a total of 139840 photons as background noise.

Figure 8(a) shows that photon energy exists when the system's incident energy is 20 keV. The main points of the energy spectrum are as follows: Cu's Kα characteristic line, 8.04 keV; Cu's Kβ characteristic line, 8.9 keV; and bremsspectrum, <20 keV. The photon flow density is about 470 counts/s. The photon time information follows a normal distribution. The expectation and variance are 470 and 53, respectively.

The arrival time of pulses and time information of background noise are mixed without energy information to produce a pulse profile (Fig. 9(a)).

SNR analysis of pulse profile with background noise

To acquire a pulse profile with high SNR, photons whose energy is in the background noise area are omit-

ted. The relationship between the deleted range and SNR is presented in Table 2. The SNR is higher when the deleted area is closer to the energy area of the background noise. When the deleted area is in the range [8, 9] keV, the SNR of the pulse profile reaches the maximum of 7.25. The pulse profile is shown in Fig. 9(b). The pulse profile SNR in Fig. 9(a) is better than that in Fig. 9(b). Background noise photon energy is concentrated in the area [8, 9] keV, although only a few signal photons are located in this area. Therefore, photon removal in the area [8, 9] keV produces the best SNR pulse profile.

Table 2.   Relationship between deleted range and SNR.

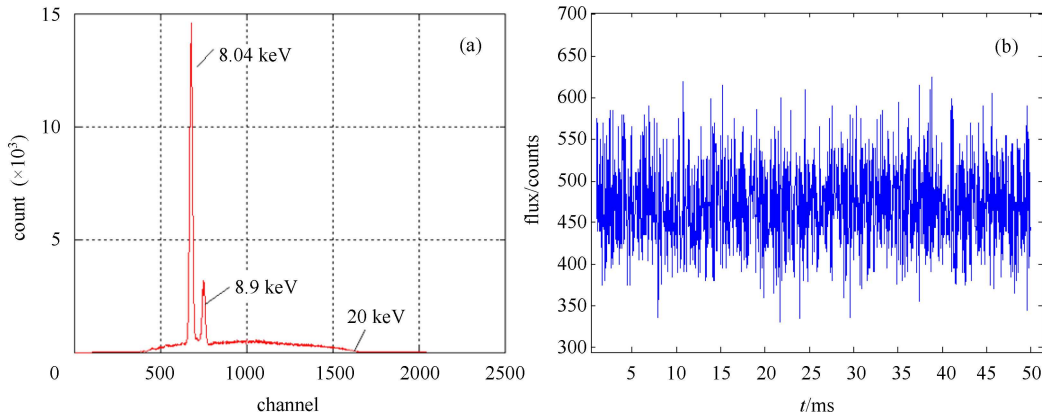| deleted range/keV	[5.3, 9]	[6.5, 9]	[7, 9]	[8, 9]	[8.5, 9]
SNR	3.79	5.01	6.25	7.25	2.35

Fig. 8.   (a) Energy spectrum of noise; (b) noise density.
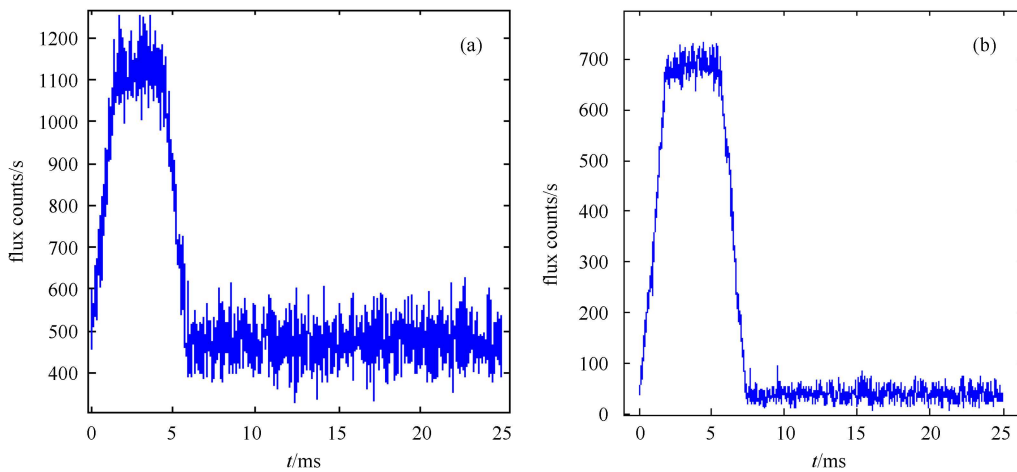

Fig. 9.   (a) Pulse profile with background noise; (b) pulse profile after eliminating photons and noise in the range [8, 9] keV.

4   Conclusions

In summary, a measurement system for X-ray photon energy and arrival time has been proposed and built. The results of performance tests show that the system can measure the energy and time precisely and satisfy requirements for navigation. We employ energy resolution and time measurement to exclude most background noise, and acquire a pulse profile with high SNR. This measurement system can be applied in autonomous navigation based on X-ray pulsars.

References

1 Voges W, Aschenbach B, Boner T et al. ROSAT All-sky Survey Faint Source Catalogue. International Astronomical Union Circular, 2000, 7432
2 Sheikh S I, Pines J D. Journal of Guidance, Control, and Dynamics, 2006, **19**: 49–63
3 Emadzadeh A A, Speye J L, Hadaegh F Y. A Parametric Study of Relative Navigation using Pulsars. Proceedings of ION 63rd Annual Meeting Cambridge, USA. 2007
4 Graven P H, Collins J T, Suneel I S et al. Spacecraft Aviation Using X-Ray Pulsars. 7th International ESA Conference on Guidance, Navigation & Control Systems. County Kerry, Ireland, 2008
5 Wood K S, Determan J R, Ray P S et al. Using the Unconventional Stellar Aspect (USA) Experiment on ARGOS to Determine Atmospheric Parameters by X-ray Occultation. Proceedings of SPIE-The International Society for Optical Engineering. USA: SPIE, 2002
6 HU Hui-Jun, ZHAO Bao-Sheng. Acta Phys. Sin., 2012, **61**(1): 1–7
7 ZHANG Fei, WANG Huan-Yu, PENG Wen-Xi et al. CPC (HEP & NP), 2012, **36**(2): 146–150
8 Lechner P, Eckbauer S, Hartmann R et al. Nuclear Instruments and Methods in Physics Research, 1996, **377**: 346–351
9 Nouais D, Beole S, Bondila M et al. Nuclear Instruments and Methods in Physics Research, 2003, **501**: 119–125
10 ZHENG Wei, SUN Shou-Ming. China Patent, ZL201010022035.7 2012 (in Chinese)